Volume 23, No 4 | International Journal of Radiation Research, October 2025

Dosimetric and biological evaluation of respiratory motion effects on dose distribution in lung cancer SIB-SBRT

L. Liu[1,2], Z. Fei[3], X. Pei[4], Q. Ren[4], J. Li[1,2], X. Cui[2*], H. Wang[1,2*]

[1]*University of Science and Technology of China, Hefei, 230026, Anhui, China*
[2]*Hefei Cancer Hospital of CAS, Institute of Health and Medical Technology, Hefei Institutes of Physical Science, Chinese Academy of Sciences, Hefei, 230031, Anhui, China*
[3]*Department of Radiation Oncology, The 901st Hospital of Joint Logistics Support Force of the Chinese People's Liberation Army, Hefei, 230031, Anhui, China*
[4]*Technology Development Department, Anhui Wisdom Technology Company Limited, Hefei, 230000, Anhui, China*

► ***Original article***

Corresponding authors:
Xiangli Cui, M.D.,
Hongzhi Wang, M.D.
E-mail:
xlcui@cmpt.ac.cn
wanghz@hfcas.ac.cn

Received: May 2024
Final revised: January 2025
Accepted: April 2025

Int. J. Radiat. Res., October 2025; 23(4): 927-934

DOI: 10.61186/ijrr.23.4.14

Keywords: *Lung neoplasms, stereotactic body radiotherapy, four-dimensional computed tomography, respiratory motion.*

ABSTRACT

Background: Simultaneous integrated boost-stereotactic body radiotherapy (SIB-SBRT) is an effective technique for lung cancer treatment but is significantly affected by respiratory motion. This study employed a four-dimensional (4D) dose calculation method to evaluate the impact of respiratory motion on dose delivery. ***Materials and Methods:*** Retrospective analysis was performed on data from 17 lung cancer patients who underwent four-dimensional computed tomography (4DCT). Volumetric modulated arc therapy (VMAT) plans, referred to as the original plans, were designed with dose prescriptions of 6 Gy per fraction for the internal target volume (ITV) and 5 Gy per fraction for the planning target volume (PTV). Control points (CPs) and monitor units (MUs) from the original plans were mapped onto ten respiratory phases of the 4DCT to generate sub-plans. These sub-plans were combined to form a 4D dose plan, followed by evaluation of physical and biological dose effects. ***Results:*** Compared to the original plans, respiratory motion reduced V100 by 1.4% for the ITV and 3.5% for the PTV. Additionally, it decreased the tumor control probability (TCP) by 0.1% for the ITV and 4.2% for the PTV. Gamma analysis revealed hot spots at the target periphery and cold spots within the target. ***Conclusion:*** Respiratory motion has a greater impact on PTV than ITV in SIB-SBRT. Dose deviations and distribution should be considered to enhance treatment accuracy.

INTRODUCTION

Lung cancer is a leading cause of cancer-related morbidity and mortality globally [1]. Stereotactic body radiation therapy (SBRT) is the preferred treatment for medically inoperable patients [2, 3] and, in some cases, for operable patients [4]. Compared to conventional radiation therapy, SBRT offers advantages such as shorter treatment durations and higher radiation doses, leading to improved biological effectiveness and superior local tumor control rates [5].

Despite its benefits, SBRT presents challenges due to steep dose gradients and reduced dose uniformity, increasing the risk of complications. The maximum dose to the planning target volume (PTV) is typically recommended to range between 110% and 140% of the prescribed dose [6]. However, achieving an optimal dose distribution within the primary tumor region is complex, as SBRT delivery techniques have limited control over the precise localization of dose hot spots.

Hypoxia within the primary tumor is a key factor in tumor relapse, as it is linked to radioresistance. Most relapses occur in the primary tumor region, primarily due to insufficient dose coverage [7]. To address dose heterogeneity within tumors, the Simultaneous Integrated Boost (SIB) technique was developed [5]. This method allows precise dose modulation, delivering higher doses to hypoxic regions of the primary tumor while sparing subclinical tumor regions and adjacent normal tissues. By optimizing dose distribution, the SIB technique enhances the therapeutic ratio and improves treatment outcomes [8].

Simultaneous integrated boost-stereotactic body radiotherapy (SIB-SBRT) requires precise delivery of high dose gradients inside and outside the PTV for optimal efficacy. However, movements such as heartbeat, gasping, coughing, and respiratory motion can significantly affect this method. Respiratory motion is the primary geometric uncertainty

[DOI: 10.61186/ijrr.23.4.14]

impacting thoracic radiotherapy accuracy, especially in lung tumors. Erridge [9] reported lung tumor motion amplitudes of up to 3.0 cm, which can affect both tumor and organ-at-risk (OAR) doses. To manage tumor motion, techniques such as abdominal compression and breath-holding are used to limit movement, whereas respiratory gating and real-time tracking enable adjustments that do not interfere with breathing [10]. Although these methods are effective, they can decrease patient comfort and increase the complexity of treatment.

A major challenge is the assumption of a consistent phase relationship between radiation delivery and breathing, as fluctuations in breathing can lead to discrepancies between the planned and actual doses. The four-dimensional (4D) dose calculation method, utilizing 4DCT imaging, captures tumor position and shape changes during respiration. By integrating tumor motion into dose calculations, the 4D dose method improves the spatial and temporal accuracy of radiation delivery, enhancing treatment precision [11, 12].

Since dosimetric dose does not always correspond directly to biological effects [13], this study utilizes Tumor Control Probability (TCP), Normal Tissue Complication Probability (NTCP), and Equivalent Uniform Dose (EUD) to provide a more accurate assessment of clinical outcomes. These metrics provide a comprehensive evaluation of therapeutic efficacy and potential risks to surrounding healthy tissues.

This study presents a 4D dose method that integrates biological evaluation to assess the impact of respiratory motion on dose delivery. By linking phase and dose information through the respiratory waveform, it provides a precise evaluation of the actual radiation dose delivered during free breathing. This approach enhances understanding of dynamic dose distribution and its biological effects, improving radiotherapy planning accuracy and minimizing risks to healthy tissues.

METHODS AND MATERIALS

Patients

This retrospective study was approved by the Ethics Committee of Hefei Cancer Hospital, Chinese Academy of Sciences (acceptance date and number: 10/28/2024; PJ-KYSQ2024-008). A total of 17 lung cancer patients (table 1) who underwent 4DCT scans and SIB-SBRT between January 2020 and December 2022 were selected for this study. The cohort included 5 males and 12 females, aged 40 to 86 years, with a median age of 63. Tumors were located in the left lung in 6 patients and the right lung in 11, with volumes ranging from 1.1 cm^3 to 58.0 cm^3. Based on the 8th edition of the American Joint Committee on Cancer (AJCC) staging system, 3 patients were classified as stage I, while 14 were classified as stage IV. The maximum motion in the left-right (LR), superior-inferior (SI), and anterior-posterior (AP) directions (LSA motion) was measured using 4DCT coordinates, with values ranging from 0.2 cm to 1.5 cm. The 3D tumor motion [14] was calculated as 3D tumor motion = $(LR^2 + AP^2 + SI^2)^{1/2}$, ranging from 0.2 cm to 1.7 cm. The center of GTV-to-diaphragm distance (GTV-D) refers to the vertical distance from the tumor center to the ipsilateral diaphragm, ranging from 1.7 cm to 17.6 cm.

Table 1. Patient demographic information.

Category	Value	Percentage (%)
Sex		
Male	5	29.4
Female	12	70.6
Age		
Median	63	
Range	40-86	
Tumor location		
Left lung	6	35.3
Right lung	11	64.7
Stage		
I	3	17.6
IV	14	82.4

Image acquisition and treatment planning

A CT simulator (Brilliance Big Bore 16-slice, Philips, Amsterdam, Netherlands) was used for 4DCT acquisition. Patients were positioned with a vacuum cushion. The scanned images were transferred to the Monaco treatment planning system (version 5.11, Elekta Medical System, Sweden) for AIP and MIP reconstructions. The ITV was contoured on the MIP dataset, transferred to AIP [15, 16], and a 5 mm margin was added to create the PTV. OARs, including the lungs, spinal cord, heart, and chest wall (CW), were outlined. Dose was prescribed as 60 Gy in 10 fractions (6 Gy/fraction) to the ITV and 50 Gy in 10 fractions (5 Gy/fraction) to PTV. Volumetric modulated arc therapy (VMAT) plans (the original plans) were created using 6 MV FF photons with the Monte Carlo dose calculation algorithm. All patients were planned with a single arc. During dose calculation and optimization, the statistical uncertainty for Monte Carlo dose calculation was 1.0% per calculation. The minimum segment width was set to 0.5 cm, with 100 control points, and the dose calculation grid was 0.1 cm. Treatment was delivered using a linear accelerator (Infinity, Elekta Medical Systems, Sweden), equipped with a 160-leaf multi-leaf collimator (MLC) with a 0.5 cm leaf width at the isocenter [17]. Figure 1 shows the treatment planning for a lung cancer patient, with the structures (ITV, PTV and OARs) outlined. The isodose color wash representing different dose levels is also shown.

4D dose plan

The log files from the linear accelerator provide control points (CPs) and their corresponding monitor units (MUs). These CPs and MUs are mapped to

[DOI: 10.61186/ijrr.23.4.14]

specific respiratory phases based on the respiratory curve, generating sub-plans for each phase. For each sub-plan, only the dose contributions from active CPs are considered, while other treatment parameters remain unchanged. The resulting sub-plans are then deformably registered and combined using AccuContour™ software (version 3.1, Xiamen Manteia Technology Ltd., China) to produce the final 4D dose plan.

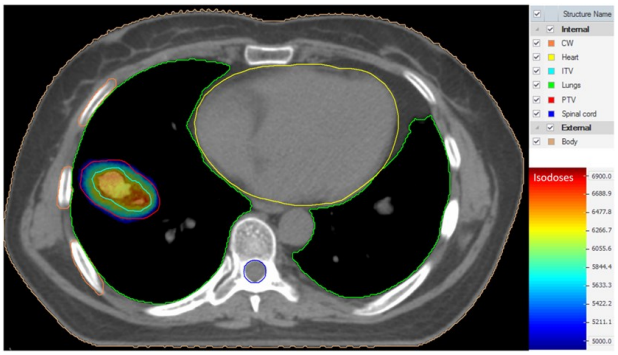

Figure 1. Treatment planning for a lung cancer patient. ITV (Internal Target Volume): light blue contour; PTV (Planning Target Volume): red contour; CW (Chest Wall): orange contour; Heart: yellow contour; Lungs: green contour; Spinal cord: dark blue contour; Body: brown contour. The isodose color wash represents the distribution of radiation doses within the PTV. Different colors indicate various dose levels, with higher doses represented by warmer colors (red and yellow) and lower doses represented by cooler colors (blue).

Dosimetric evaluation

The dosimetric parameters of the target ITV, PTV, and OARs were analyzed for both the original plan and the 4D dose plan. The key parameters for evaluating the target included the volume receiving 100% of the prescribed dose (V_{100}), the dose to 95% of the target volume (D_{95}), minimum (D_{min}), maximum (D_{max}), and mean dose (D_{mean}), as well as the heterogeneity index (HI) [18], conformity index (CI) [19], and gradient index (GI) [20].

The OARs dosimetric parameters were evaluated as follows: (1) Lungs V_5: percentage of lung volume receiving 5 Gy; (2) Lungs V_{20}: percentage receiving 20 Gy; (3) Lungs V_{30}: percentage receiving 30 Gy; (4) Lungs Dmean: mean lung dose; (5) Heart D_{max}: maximum heart dose; (6) Heart D_{mean}: mean heart dose; (7) CW D_{max}: maximum chest wall dose; (8) Spinal Cord D_{max}: maximum spinal cord dose.

Biological evaluation

The TCP of ITV and PTV was used to assess tumor control, while the NTCP for the Lungs, Heart, Spinal cord, and CW predicted organ toxicity. Both TCP and NTCP were calculated using the Niemierko model based on the equivalent uniform dose (EUD) and the EQD_2 equation [21, 22].

The TCP and NTCP values were calculated using an improved program based on Gay's method [23] with MATLAB (version 9.10, MathWorks, USA). The calculation process involved: (1) Exporting statistics from the cumulative dose-volume histogram (cDVH) of the ITV, PTV, lungs, heart, spinal cord, and CW at a 5 cGy resolution into MATLAB. (2) Converting the cDVH into a differential dose-volume histogram (dDVH) with Gay's method. (3) Converting the dose in each volume element to the EQD_2. (4) Calculating TCP and NTCP values using parameters listed in table 2. Normal tissue tolerance parameters (a, γ_{50}, and TD_{50}) were taken from Emami [24] and Deepak [21], while TCP parameters were based on Niemierko [25].

Table 2. The parameters of the formulas.

	TCP	$NTCP_{Lungs}$	$NTCP_{Heart}$	$NTCP_{Spinalcord}$	$NTCP_{CW}$
TCD_{50}(Gy)	51.97	--	--	--	--
TD_{50} (Gy)	--	24.5	48	66.5	68
α/β	10	3	3	3	3
a	-10	1	3	13	10
γ_{50}	1.81	2	3	--	--
Endpoints		Pneumonitis	Pericarditis	Myelitis/ necrosis	Pathologic fracture

Abbreviations: TCP:Tumor Control Probability; NTCPLungs: Normal Tissue Complication Probability for the lungs; NTCPHeart: Normal Tissue Complication Probability for the heart; NTCPSpinalcord: Normal Tissue Complication Probability for the spinal cord; NTCPCW: Normal Tissue Complication Probability for the chest wall; TCD50: Dose required to achieve a 50% probability of tumor control with homogeneous irradiation; TD50: Whole organ dose at which NTCP is 50%; α/β: Parameter from the issue-specific LQ (Linear-Quadratic) model, determining the fractionation sensitivity; a: Tissue-specific parameter describing the volume effect; γ50: Slope of the sigmoidal dose-response curve for the tumor. --: If the parameter γ50 was not available, a default value of 4 was used.

Statistical analysis

The data were presented as medians accompanied by interquartile ranges (IQRs). Statistical evaluations were performed using SPSS (version 25, IBM Corp., Armonk, NY, USA). Differences between variables were analyzed using the Wilcoxon signed-rank test, and statistical significance was determined at a two-tailed p-value threshold of less than 0.05.

The Spearman correlation coefficient was used to analyze the correlation between variables and V_{100} reduction, performed in GraphPad Prism (version 8.0.2, GraphPad Software Inc., San Diego, CA, USA). The coefficient (r) varies between -1 and 1, where $r>0$ signifies a positive relationship, $r<0$ indicates a negative relationship, and larger absolute values of $|r|$ represent stronger correlations.

Verisoft software (version 5.1, PTW Freiburg GmbH, Freiburg, Germany) was utilized to perform a 3D gamma analysis, employing criteria of a 1% dose variation and a 1 mm distance-to-agreement, to assess the consistency between the original plan and the 4D dose plan.

RESULTS

Effect of respiratory motion on dosimetric dose

Table 3 shows the statistical differences in dose parameters (V_{100}, D_{95}, D_{min}, D_{max}, D_{mean}) and indices (HI, CI, GI) between the original plan and 4D dose plan for ITV and PTV. The differences, calculated as the relative change between the 4D dose plan and the

[DOI: 10.61186/ijrr.23.4.14]

original plan, are reported as median values with interquartile ranges (IQR) and p-values indicating statistical significance.

The 4D dose plan resulted in reductions in key dose metrics for both ITV and PTV. For ITV, V_{100} decreased slightly from 98.8% to 97.4% (p=0.007), and D_{95} dropped from 61.1 Gy to 60.6 Gy (p=0.002). For PTV, the reductions were more pronounced, with V_{100} decreasing from 98.1% to 93.8% (p<0.001) and D_{95} from 52.2 Gy to 49.4 Gy (p<0.001). Similarly, D_{mean} decreased from 63.9 Gy to 63.1 Gy for ITV (p<0.001) and from 60.0 Gy to 58.4 Gy for PTV (p<0.001). D_{max} showed significant reductions for both targets, dropping from 68.6 Gy to 66.4 Gy (p<0.001).

Plan quality indicators improved or remained stable. The CI improved for ITV from 0.6 to 0.7 (p<0.001) and remained constant for PTV at 0.8 (p=0.003). The GI decreased significantly for both targets, from 10.4 to 9.7 for ITV and from 5.5 to 5.3 for PTV (p<0.001). HI remained stable for ITV (1.1, p=0.718) and for PTV (1.3, p=0.001).

Table 3. Statistical comparison of target dose metrics between original plan and 4D dose plan for ITV and PTV.

	ITV				PTV			
	Original plan	4D dose method	Differences	p	Original plan	4D dose method	Differences	p
V_{100} (%)	98.8(1.2)	97.4(3.9)	-1.4(4.5)	0.007	98.1(1.7)	93.8(5.1)	-3.5(4.2)	< 0.001
D_{95} (Gy)	61.1(0.5)	60.6(1.0)	-1.0(2.0)	0.002	52.2(1.1)	49.4(2.4)	-4.2(4.0)	< 0.001
D_{min} (Gy)	57.7(2.3)	56.9(3.1)	-1.6(3.4)	0.076	43.2(6.4)	38.4(7.0)	-6.1(11.7)	0.004
D_{max} (Gy)	68.6(2.2)	66.4(1.6)	-3.2(1.0)	< 0.001	68.6(2.2)	66.4(1.6)	-3.2(1.0)	< 0.001
D_{mean}(Gy)	63.9(1.1)	63.1(0.9)	-1.0(1.0)	< 0.001	60.0(1.2)	58.4(0.8)	-2.1(2.0)	< 0.001
HI	1.1(0.0)	1.1(0.0)	0.0(1.4)	0.718	1.3(0.1)	1.3(0.1)	3.1(3.5)	0.001
CI	0.6(0.2)	0.7(0.2)	12.1(13.5)	< 0.001	0.8(0.2)	0.8(0.1)	3.6(5.2)	0.003
GI	10.4(9.8)	9.7(9.1)	-2.8(3.3)	< 0.001	5.5(2.5)	5.3(2.6)	-4.1(2.8)	< 0.001

Abbreviations: ITV: Internal Target Volume; PTV: Planning Target Volume; V100: the volume receiving 100% of the prescribed dose; D95:the dose to 95% of the target volume; Dmax: maximum dose; Dmin: minimum dose; Dmean: mean dose; HI: Heterogeneity Index; CI: Conformity Index; GI: Gradient Index.

Table 4 presents statistical comparison of OARs dose metrics between original plan and 4D dose plan. The 4D dose plan effectively reduced high-dose exposure to the lungs, with V_{20} and V_{30} decreasing by 1.7% (p = 0.004) and 2.0% (p<0.001), respectively, while maintaining a stable D_{mean} at 3.9 Gy (p=0.004). V_5 increased slightly to 17.3% (p=0.007), with minimal clinical impact. CW and heart D_{max} were reduced to 51.7 Gy and 19.7 Gy (p=0.004, p=0.001), with heart D_{mean} unchanged at 2.4 Gy. Spinal cord D_{max} dropped significantly to 11.8 Gy (p<0.001), reducing the risk of radiation injury.

Table 4. Statistical comparison of OARs dose metrics between original plan and 4D dose plan.

OARs		Original plan	4D dose method	Differences (%)	p
Lungs	V_5 (%)	16.8(9.4)	17.3(9.8)	-1.0(1.7)	0.007
	V_{20} (%)	5.9(5.2)	5.6(5.1)	-1.7(3.2)	0.004
	V_{30} (%)	3.1(2.8)	3.0(2.8)	-2.0(3.6)	<0.001
	D_{mean}(Gy)	3.9(2.4)	3.9(2.4)	-0.6(0.9)	0.004
CW	D_{max}(Gy)	53.8(30.6)	51.7(28.7)	-3.2(2.6)	0.004
Heart	D_{max}(Gy)	20.4(28.0)	19.7(25.0)	-4.2(7.7)	0.001
	D_{mean}(Gy)	2.4(4.3)	2.4(4.2)	0.0(0.0)	0.932
Spinal cord	D_{max}(Gy)	12.2(8.4)	11.8(8.0)	-4.2(2.5)	<0.001

Abbreviations: OAR: Organ-At-Risk; Vxx: percentage of OAR receiving xx Gy; Dmax: maximum dose; Dmin: minimum dose; Dmean: mean dose.

Effect of respiratory motion on dose distribution

Select data from the patient with the largest 3D tumor motion to analyze the impact of respiratory motion on dose distribution. Figure 2 compares dose distributions between the original and 4D dose plans. Figure 2A shows reduced high-dose coverage in the 4D plan, with constricted 90% and 80% isodose lines and expanded 50% and 20% lines along the SI direction. Figure 2B presents 3D gamma analysis, highlighting dose deviations due to respiratory motion, with hot spots at the target edges and cold spots within the target, potentially compromising tumor coverage and increasing OAR toxicity.

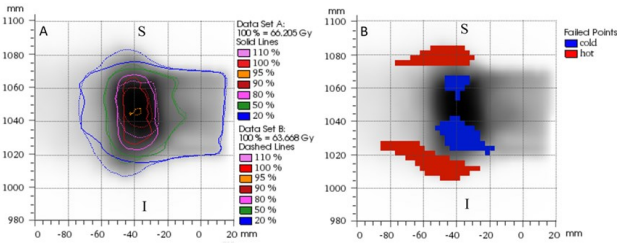

Figure 2. Comparison of dose distribution between the original plan and the 4D dose plan. **(A)** Isodose distribution: Data Set A (solid lines) shows the original plan, and Data Set B (dashed lines) represents the 4D dose plan. Isodose lines (20% -110%) highlight dose coverage variations. **(B)** 3D Gamma analysis: Blue indicates underdosage ("cold spots") and red shows overdose ("hot spots"). S: Superior; I: Inferior.

Table 5 shows gamma pass rates at various dose levels in the sagittal plane for the 4D dose plan. At the 3%/3mm criteria, pass rates are high, ranging from 97.3% at the 10% dose level to 100% at the 100% dose level. At the 2%/2mm criteria, pass rates decrease slightly, from 94.6% to 100%. The 1%/1mm criteria show a greater decline, with rates ranging from 58.5% at the 70% dose level to 88.2% at 100%. These results indicate that respiratory motion causes dose deviations, with smaller tolerance levels leading to a more noticeable impact, especially at lower dose levels.

[DOI: 10.61186/ijrr.23.4.14]

Table 5. Gamma pass rate at various dose levels in the sagittal plane for 4D dose plan.

Dose level (%)	3%3mm	2%2mm	1%1mm
10	97.3%	94.6%	87.3%
30	97.5%	93.7%	84.6%
50	95.6%	87.5%	70.7%
70	90.7%	81.4%	58.5%
80	91.3%	82.6%	58.9%
85	93.3%	85.7%	62.2%
90	95.6%	89.8%	65.9%
95	99.3%	97.4%	76.5%
100	100.0%	100.0%	88.2%

Interfering factors contributing to dosimetric dose reductions

Data analysis revealed variability in dose deviations caused by respiratory motion across patients. A correlation analysis was performed to identify factors contributing to dose reductions, focusing on ITV and PTV volumes, motion ranges in LR, SI, and AP directions, LSA motion, GTV-D, and 3D tumor motion. Using the Spearman correlation coefficient, the analysis showed strong correlations between GTV-D (r=-0.7468, p=0.0009 for ITV; r=-0.5972, p=0.0129 for PTV), LSA motion (r=0.8302, p<0.0001 for ITV; r=0.6759, p=0.0036 for PTV), and 3D tumor motion (r=0.8643, p<0.0001 for ITV; r=0.7551, p<0.0007 for PTV) with reductions in V_{100}.

Figure 3 shows linear regression analysis of V_{100} reduction for ITV and PTV against three factors: 3D tumor motion, LSA motion, and GTV-D. 3D tumor motion shows strong positive correlations with V_{100} reduction for both ITV (R^2=0.8074, p<0.0001) and PTV (R^2=0.5551, p=0.0006). LSA motion has a stronger effect on ITV (R^2=0.7951, p<0.0001) than on PTV (R^2=0.4962, p=0.0016). GTV-D shows a negative correlation with V_{100}, with greater distance leading to reduced dose coverage for both targets (ITV: R^2=0.4025, p=0.0062; PTV: R^2=0.5432, p=0.0007).

Effect of respiratory motion on biological dose

Table 6 compares TCP, NTCP, and EUD for the ITV, PTV, and OARs, including the lungs, heart, spinal cord, and CW, with differences reported as median (IQR) and p-values for statistical significance. The 4D dose method reduced TCP and EUD for the PTV, with TCP dropping from 96.9% to 92.7% and EUD from 83.6 Gy to 73.9 Gy. In contrast, the reductions for the ITV were less pronounced. For OARs, NTCP for the lungs, heart, and spinal cord remained negligible under both plans, while NTCP for the CW significantly decreased from 27.4% to 14.9% with the 4D dose method.

Table 6. Comparison of biological dose metrics between original and 4D dose calculation plans.

	Original	4D dose method	Differences	p
TCP_{ITV} (%)	99.2(0.2)	99.0(0.4)	-0.1(0.2)	0.001
TCP_{PTV} (%)	96.9(1.3)	92.7(5.5)	-4.2(4.8)	<0.001
$NTCP_{lungs}$ (%)	0.0(0.0)	0.0(0.0)	0.0(0.0)	--
$NTCP_{heart}$ (%)	0(0)	0(0)	0.0(0.0)	--
$NTCP_{spinalcord}$ (%)	0(0)	0(0)	0.0(0.0)	--
$NTCP_{CW}$ (%)	27.4(100)	14.9(100)	0.0(55.1)	0.043
EUD_{ITV} (Gy)	101(2.4)	98.5(3.0)	-2.0(3.0)	0.001
EUD_{PTV} (Gy)	83.6(4.8)	73.9(9.7)	-10.0(8.3)	<0.001
EUD_{lungs} (Gy)	4.6(3.4)	4.2(3.3)	-4.6(4.4)	<0.001
EUD_{heart} (Gy)	2.8(3.6)	2.7(3.4)	-4.7(3.2)	0.002
$EUD_{spinalcord}$ (Gy)	3.3(2.9)	3.2(2.9)	-1.9(2.4)	<0.001
EUD_{CW} (Gy)	64.0(106.7)	61.0(102.5)	-3.7(3.9)	0.001

Abbreviations: TCP: Tumor Control Probability; NTCP: Normal Tissue Complication Probability; EUD: Equivalent Uniform Dose.

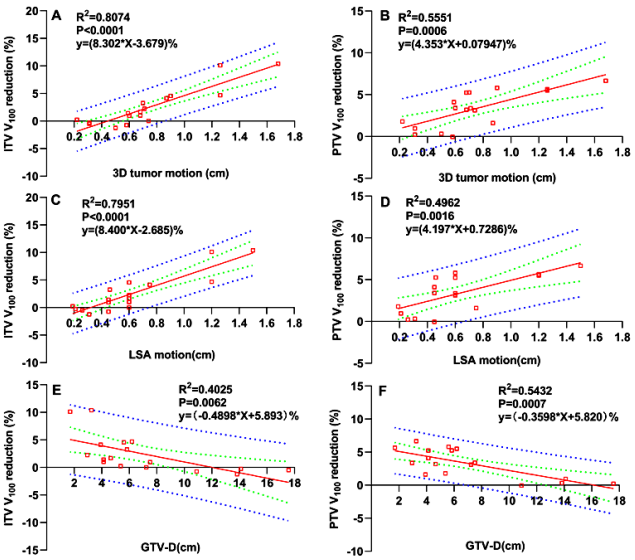

Figure 3. Linear regression analysis between V100 reductions for ITV (Internal Target Volume) and PTV (Planning Target Volume) and three key factors: 3D tumor motion, LSA motion (the maximum motion in the left-right (LR), superior-inferior (SI), and anterior-posterior (AP) directions), and GTV-D (the center of GTV-to-diaphragm distance). The plots illustrate the correlations, with R2 values and regression equations indicating the strength and nature of these relationships. Red lines represent linear fits, green dots are 95% confidence bands, and blue dots are 95% prediction bands.

DISCUSSION

SIB-SBRT effectively delivers differential doses to high-risk regions within the tumor while preserving surrounding normal tissues, improving therapeutic outcomes and reducing recurrence rates. However,

[DOI: 10.61186/ijrr.23.4.14]

respiratory motion presents a significant challenge to dose accuracy, necessitating a thorough assessment of its effects on this precision therapy. To address this, the study employs a 4D dose calculation method, providing a comprehensive analysis of the dosimetric and biological impacts of respiratory motion on both ITV and PTV.

Respiratory motion reduces high-dose coverage in both ITV and PTV, which directly impacts tumor control and normal tissue toxicity. For ITV, slight decreases in V_{100} and significant reductions in D_{max} and D_{mean} indicate compromised dose delivery, particularly in high-dose regions. This highlights the challenge of maintaining uniform dose coverage, especially for ITV, which is more sensitive to respiratory motion due to its smaller volume and higher precision requirements. In contrast, PTV experienced a larger reduction in dose coverage, demonstrating the increased sensitivity of larger targets to motion-induced deviations. While the impact on normal tissue dose values was minimal, it remains significant. These findings are consistent with Li's study [26], which reported a decrease in PTV V_{100} coverage from 0.7% to 15.4% as respiratory motion increased from 0.5 cm to 1.6 cm, with minimal differences between 3D and 4D dose calculations for GTV. Previous studies [27-29] have also explored the impact of respiratory motion on dose distribution. Chang *et al.* [27] found that respiratory motion affects the overall dose in IMRT, aligning with our findings. Respiratory motion disrupts dose homogeneity, creating hot spots at the periphery and cold spots within the target area. These trends, also observed in other research [28, 29], are more pronounced in SIB-SBRT, potentially leading to greater dose heterogeneity.

While dosimetric changes underscore significant reductions in target coverage, biological dose analysis reveals the associated impact on tumor control and normal tissue toxicity. Respiratory motion results in a reduced TCP for PTV, consistent with dosimetric findings, particularly the decreases in V_{100} and D_{95}. These dose reductions demonstrate that larger target volumes experience greater loss of tumor control due to respiratory motion. Moreover, EUD values for both ITV and PTV decreased, with a more pronounced reduction for PTV, further indicating compromised dose delivery. While the NTCP for the lungs, heart, and spinal cord remained unchanged, suggesting no increase in toxicity for these organs, the NTCP for the chest wall significantly decreased, indicating a reduced risk of toxicity for this structure.

Patient variability in dose reductions emphasizes the importance of considering several factors affecting dosimetric outcomes. GTV-D, LSA motion, and 3D tumor motion were strongly correlated with reductions in V_{100} for both ITV and PTV. Notably, larger GTV-D distances were negatively correlated with dose coverage, particularly for PTV, suggesting that smaller distances from the diaphragm exacerbate respiratory motion's impact on dose distribution. These results emphasize the need for individualized treatment plans. The strongest correlation was found between 3D tumor motion and V_{100} reduction, particularly for ITV, highlighting the importance of accounting for tumor motion in treatment planning. Additionally, the stronger effect of LSA motion on ITV compared to PTV further emphasizes the critical role of lateral and superior-inferior tumor movements in driving dose deviations. Using 5% deviation thresholds for clinical doses, specific thresholds for respiratory motion management were identified: 3D tumor motion > 1.1 cm, LSA > 1.0 cm, or GTV-D < 1.8 cm. Exceeding these thresholds necessitates tailored motion management to optimize treatment precision. Liu *et al.* [30] emphasized careful planning when the breathing curve exceeds 1.0 cm. Ohira *et al.* [31] explored dose discrepancies for tumors near the diaphragm but did not quantify tumor-to-diaphragm distance. Ehrbar *et al.* [32] reported dose differences in the GTV of less than 3.8%. Our findings align with these studies and provide additional data support, emphasizing the need for customized treatment strategies.

By using a 4D dose calculation method, this study provides a more accurate reflection of the effects of respiratory motion on dose delivery, overcoming the limitations of traditional static dose calculations. Our analysis highlights the increased sensitivity of larger PTV volumes to respiratory motion, resulting in substantial reductions in dose coverage for large tumor target volumes. These findings provide a foundation for developing personalized treatment plans, especially for patients with significant respiratory motion or tumors near the diaphragm. In terms of normal tissue toxicity, biological dose analysis suggests that although respiratory motion decreases TCP, it does not significantly increase toxicity risks to normal tissues. The study also establishes thresholds for respiratory motion management based on correlation analysis. When 3D tumor motion exceeds 1.1 cm, LSA exceeds 1.0 cm, or GTV-D is less than 1.8 cm, appropriate management strategies should be applied. These thresholds offer practical guidance for optimizing treatment precision while minimizing normal tissue damage in clinical practice.

Future research should focus on refining respiratory motion management in radiotherapy, particularly through larger, prospective clinical trials across diverse patient populations. Investigating the effects of additional motion management techniques, such as real-time tumor tracking or gating methods, alongside 4D dose calculations, could provide deeper insights into minimizing dose deviations. Future studies should also explore the effects of Hounsfield Unit (HU) variations and the interplay between tumor

[DOI: 10.61186/ijrr.23.4.14]

motion and radiation delivery. More detailed analysis of how breathing patterns and tumor characteristics influence dose coverage could lead to better treatment outcome predictions. Lastly, optimizing the balance between tumor control and normal tissue toxicity remains crucial for improving long-term outcomes in lung cancer SIB-SBRT.

CONCLUSION

Respiratory motion disrupts dose homogeneity in SIB-SBRT, reducing target coverage and increasing variability, particularly for tumors with large motion amplitudes or those near the diaphragm. Effective motion management is crucial to optimizing dose delivery, preserving tumor control, and minimizing normal tissue toxicity. Tailored strategies, including advanced imaging and motion compensation, are essential for improving treatment precision.

Acknowledgements: None.

***Ethics consideration*:** This retrospective study was approved by the Ethics Committee of Hefei Cancer Hospital, Chinese Academy of Sciences (acceptance date and number: 10/28/2024; PJ-KYSQ2024-008).

***Competing interests*:** Declared None.

***Funding*:** This work was supported by the National Science Foundation of China (No.82202945), Nature Science Research Project of Anhui Province (No.2208085MA13) and Health Research Program of Anhui (AHWJ2024Ab0178).

***Authors' contributions*:** L.L.: participation in the whole work; drafting of the article; collected the 4DCT data; data analysis. X.C. and H.W.: writing review & editing. Z.F., X.P. and Q.R.: interpreted the data. J.L.: collected the logfile data.

REFERENCES

1. Sung H, Ferlay J, Siegel RL, Laversanne M, Soerjomataram I, Jemal A, *et al.* (2021) Global Cancer Statistics 2020: GLOBOCAN Estimates of Incidence and Mortality Worldwide for 36 Cancers in 185 Countries. *CA Cancer J Clin,* ***71(3)****: 209-249.*
2. Timmerman R, Paulus R, Galvin J, Michalski J, Straube W, Bradley J, *et al.* (2010) Stereotactic body radiation therapy for inoperable early-stage lung cancer. *JAMA,* ***303(11):*** *1070-1076.*
3. Bezjak A, Paulus R, Gaspar LE, Timmerman RD, Straube WL, Ryan WF, *et al.* (2016) Efficacy and toxicity analysis of NRG Oncology/ RTOG 0813 trial of stereotactic body radiation therapy (SBRT) for centrally located non-small cell lung cancer (NSCLC). *Int J Radiat Oncol Biol Phys,* ***96(2):*** *S8.*
4. Tandberg DJ, Tong BC, Ackerson BG, Kelsey CR (2018) Surgery versus stereotactic body radiation therapy for stage I non-small cell lung cancer: A comprehensive review. *Cancer*, ***124(4):*** *667-678.*
5. Zhang Q, Cai XW, Feng W, Yu W, Fu XL (2022) Dose-escalation by hypofractionated simultaneous integrated boost IMRT in unresectable stage III non-small-cell lung cancer. *BMC Cancer,* ***22 (1)****: 96.*
6. Hurkmans CW, Cuijpers JP, Lagerwaard FJ, Widder J, van der Heide UA, Schuring D, *et al.* (2009) Recommendations for implementing stereotactic radiotherapy in peripheral stage IA non-small cell lung cancer: report from the Quality Assurance Working Party of the randomised phase III ROSEL study. *Radiat Oncol,* ***4(1):*** *1-14.*
7. Kelada OJ, Decker RH, Nath SK, Johung KL, Zheng MQ, Huang YY, *et al.* (2018) High single doses of radiation may induce elevated levels of hypoxia in early-stage non-small cell lung cancer tumors. *Int J Radiat Oncol Biol Phys,* ***102(1)****: 174-183.*
8. Haque WM, Endres EC, Szeja S, Hatch SS, Joyner MM, Internationals O (2016) Simultaneous integrated boost using conformal radiation therapy for treatment of cervical cancer. *Int J Cancer,* ***3(1):*** *1-7.*
9. Tanabe Y, Deguchi T, Kiritani M, Hira N, Tomimoto S, Nishikawa H, *et al.* (2024) Evaluation of statistical prediction model fitting by combining fiducial markers and lung volume for stereotactic body radiotherapy. *Int J Radiat Res,* ***22(1)****: 17-22.*
10. Kaviarasu K, Raj NAN, Murthy KK (2021) Dosimetric evaluation of intensity modulated radiation therapy for different duty cycles of the gated beam delivery. *Int J Radiat Res,* ***19(3)****: 669-683.*
11. Chung H, Jung J, Jeong C, Kwaket J, Park J, Kim JJ, *et al.* (2018) Evaluation of delivered dose to a moving target by 4D dose reconstruction in gated volumetric modulated arc therapy. *PLoS ONE,* ***13(9):*** *e0202765.*
12. Zeng YL, Chang Y, Zhang S, Han J, Liu HY, Xiao F, *et al.* (2023) Clinical evaluation of 4D dynamic dose for thoracic tumor stereotactic body radiation therapy with variable parameters. *Radiat Med Prot,* ***4(3):*** *150-158.*
13. Kauweloa KI, Gutierrez AN, Bergamo A, Stathakis S, Papanikolaou N, Mavroidis P (2014) Practical aspects and uncertainty analysis of biological effective dose (BED) regarding its three-dimensional calculation in multiphase radiotherapy treatment plans. *Med Phys,* ***41(7):*** *071707.*
14. Karava K, Ehrbar S, Riesterer O, Roesch J, Glatz S, Klöck S, *et al.* (2017) Potential dosimetric benefits of adaptive tumor tracking over the internal target volume concept for stereotactic body radiation therapy of pancreatic cancer. *Radiat Oncol,* ***12(1)****: 175.*
15. Tian Y, Wang ZH, Ge H, Zhang T, Cai J, Kelsey C, *et al.* (2012) Dosimetric comparison of treatment plans based on free breathing, maximum, and average intensity projection CTs for lung cancer SBRT. *Med Phys,* ***39(5)****: 2754-2760.*
16. Chan MKH, Kwong DLW, Ng SCY, Tam EKW, Tong ASM. (2012) Investigation of four-dimensional (4D) Monte Carlo dose calculation in real-time tumor tracking stereotatic body radiotherapy for lung cancers. *Med Phys,* ***39(9)****: 5479-5487.*
17. Park J, Xu Q, Xue J, Zhai Y, An L, Chen Y (2014) SU-E-T-119: Dosimetric and Mechanical Characteristics of Elekta Infinity LINAC with Agility MLC. *Med Phys,* ***41(6)****: 249-249.*
18. Patel G, Mandal A, Choudhary S, *et al.* (2020) Plan evaluation indices: A journey of evolution. *Rep Pract Oncol Radiother,* ***25(3)****: 336-344.*
19. Ozturk N, Ozbek N, Depboylu B (2022) Dosimetric comparison of IMRT, VMAT and HYBRID treatment methods in radical radiation therapy of prostate cancer. *Int J Radiat Res,* ***20(2)****: 411-416.*
20. Hoffman D, Dragojević I, Hoisak J, Hoopes D, Manger R (2019) Lung Stereotactic Body Radiation Therapy (SBRT) dose gradient and PTV volume: a retrospective multi-center analysis. *Radiat Oncol,* ***14(1)****: 162.*
21. Thaper D, Singh G, Kamal R, Oinam AS, Yadav HP, Kumar R, *et al.* (2021) Impact of dose heterogeneity in target on TCP and NTCP for various radiobiological models in liver SBRT: different isodose prescription strategy. *Biomed Phys Eng Express,* ***7(1)****: 015020.*
22. Chang JH, Gehrke C, Prabhakar R, Gill S, Wada M, Joon DL, *et al.* (2016) RADBIOMOD: A simple program for utilising biological modelling in radiotherapy plan evaluation. *Phys Med,* ***32(1)****: 248-254.*
23. Gay HA and Niemierko A (2007) A free program for calculating EUD -based NTCP and TCP in external beam radiotherapy. *Phys Med,* ***23 (3-4)****: 115-125.*
24.]Emami B, Lyman J, Brown A, Coia L, Goitein M, Munzenrider JE, *et al.* (1991) Tolerance of normal tissue to therapeutic irradiation. *Int J Radiat Oncol Biol Phys,* ***21(1)****: 109-122.*
25. Chaikh A and Balosso J (2016) The use of radiobiological TCP and NTCP models to validate the dose calculation algorithm and readjust the prescribed dose. *Radiother Oncol,* ***118(1)****: S24.*
26. Li X, Yang Y, Li TF, Fallon K, Heron DE and, Huq MS (2013) Dosimetric effect of respiratory motion on volumetric-modulated arc therapy-based lung SBRT treatment delivered by TrueBeam machine with flattening filter-free beam. *J Appl Clin Med Phys,* ***14 (6)****: 4370.*
27. Chang LR, Yu XC, Lu ZW, WU B, Qi B (2015) The influence of respiratory motion on dose distribution of 3D-CRT and IMRT- a simulation study. *Int J Radiat Res,* ***13(1)****: 39-43.*
28. Palmer AL, Nash D, Kearton JR, Jafari SM, Muscat S (2017) A multicentre 'end to end' dosimetry audit of motion management (4DCT-defined motion envelope) in radiotherapy. *Radiother Oncol,*

[DOI: 10.61186/ijrr.23.4.14]

125(3): *453-458.*
29. Thomas A, Yan H, Oldham M, Juang T, Adamovics J, Yin FF (2013) The effect of motion on IMRT-looking at interplay with 3D measurements. *J Phys Conf Ser*, ***444***: *012049*.
30. Liu G, Hu F, Ding XF, *et al.* (2019) Simulation of dosimetry impact of 4DCT uncertainty in 4D dose calculation for lung SBRT. *Radiat Oncol.* ***14***: *1.*
31. Ohira S, Ueda Y, Hashimoto M, Miyazaki M, Isono M, Kamikaseda H, *et al.* (2016) VMAT-SBRT planning based on an average intensity projection for lung tumors located in close proximity to the diaphragm: a phantom and clinical validity study. *J Radiat Res,* ***57 (1)***: *91-97.*
32. Ehrbar S, Lang S, Stieb S, Riesterer O, Stark LS, Guckenberger M, *et al.* (2016) Three-dimensional versus four-dimensional dose calculation for volumetric modulated arc therapy of hypofractionated treatments. *Z Med Phys,* ***26(1)***: *45-53.*

[DOI: 10.61186/ijrr.23.4.14]